Driver-Integrated Active-Matrix Amorphous Silicon Schottky Photosensor Arrays for Display Integration

Marco M. Dettling*, Patrick Schalberger, Norbert Fruehauf

Institute for Large Area Microelectronics and Research center SCoPE, University of Stuttgart, Stuttgart Germany

Abstract

This paper shows an active-matrix Schottky photodiode-based image sensor. It is shown that amorphous silicon Schottky photodiodes may be favorable over pin-photodiodes due to their simpler and highly TFT-compatible manufacturing process, eliminating the need for a p-doping and retaining strong device performance. The device performance is shown and evaluated with regards to different applications such as ambient light sensing as well as in-screen fingerprint detection. An active-matrix sensor array is shown, featuring integrated row drivers and column multiplexing to reduce external driver circuitry such as ADC channels and to provide a scalable technology.

Photosensor, Amorphous silicon Schottky diode, Sensor array, Active-matrix configuration, Ambient light, Image sensor, Fingerprint sensor

1. Introduction

Photosensors based on amorphous silicon (a-Si:H) have been in use for many years, especially in ambient light detection of displays [1-3] or detector arrays for medical applications [4]. The most common sensor types are some form of photosensitive thin film transistors (TFT) or pin-photodiodes. However, an often-overlooked sensor is the Schottky photodiode. This device features a very simple manufacturing process, robust performance and high reproducibility in a small footprint and is thus ideal for array implementation in any TFT backplane. The process compatibility with other TFT technologies such as InGaZnO has also been shown in a previous paper [5]. This paper presents a scalable integration of a sensor array with integrated drivers and live readout. That technology enables functions such as spatial resolution of cast shadows on displays for adaptive brightness adjustment and is considered to be applicable as well for biometric functions such as on-screen fingerprint recognition.

2. Manufacturing process and device architecture

The manufacturing process for the co-fabrication of photodiodes and back channel etched (BCE) a-Si:H-TFTs is shown in more detail in [5]. Figure 1 shows the resulting layer stack that was used to fabricate all shown devices. The photodiodes consist of a bottom metal layer, and an a-Si semiconductor layer, making up the Schottky contact in the device. The top contact of the Schottky diode is realized by an n+ doped a-Si layer and ITO, to achieve a transparent electrode. Light thus enters the device from the top. Isolation of the sidewalls, as well as between top and bottom metal layers is done by a triple layer of Si_xN_y and SiO_x deposited in a single PECVD process. This layer also acts as the gate-dielectric for the TFT layer stack. The diode bottom metal layer also functions as the gate metal layer. After the formation of the TFT semiconductor layer, the drain-source deposition and the back-channel, a Si_xN_y passivating layer is deposited, followed by a TFT light shield. In order to avoid any potential negative impact of successive PECVD processes on the already deposited layers, each PECVD step was performed at a lower temperature than the previous one. The shown process requires only one additional functional layer compared to the TFT fabrication process. In a display application, the light shield would be implemented in the black-matrix on the color filter substrate. The total mask count is seven plus one for the light shield. In principle, it seems possible to further reduce the process effort by using the same semiconductor layer for the Schottky diodes and the TFTs. However, preliminary tests have shown adhesion problems of the amorphous silicon layer on top of the dielectric after the vacuum break, which is necessary for the formation of the contact holes through the dielectric to the diodes' bottom metal. Furthermore, the a-Si layer of the Schottky diodes should be relatively thick for a high light absorption, while the TFTs' a-Si layer should be thinner to avoid excessive leakage currents.

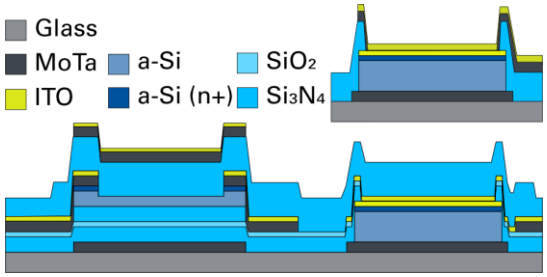

Figure 1. Layer stack of photodiode (top right) as well as co-fabricated photodiode and TFT (bottom).

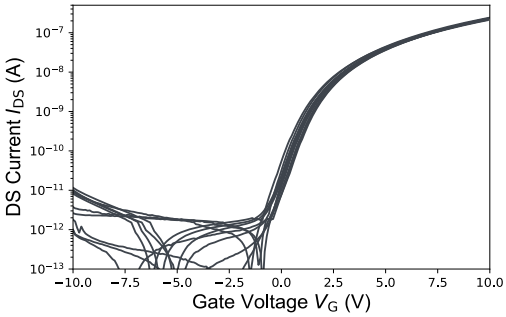

Figure 2. Input characteristic of a-Si:H-TFTs with a width and length of 10 µm and a drain-source voltage VDS = 10 V.

3. Electrical device characterization

Individual TFTs where used for device performance evaluation alongside the arrays. Figure 2 shows the measured input characteristic of TFTs with a width $w = 10\,\mu m$ and length $l = 10\,\mu m$. The extracted field effect mobility from these measurements is $0.383 \pm 0.024\,cm^2/Vs$ on average, with a threshold voltage of $1.79 \pm 0.17\,V$. The mobility of the devices is comparatively low for this technology. However, test structures

ISSN 0097-996X/25/5603-2086-$1.00 © 2025

of the row-drivers as well as the actual active-matrix still showed good functionality. The IV-characteristic of the photodiodes for different illumination levels is shown in figure 3b). Illumination was done using a green LED with a narrow spectrum at a center wavelength of 520 nm. The spectrum is shown in figure 3a) for a brightness of 1430 lux. The external quantum efficiency for this spectrum was calculated to be 38% for similar devices [5]. The photosensitive area of each sensor has a size of 32x32 µm^2. Smaller sensor areas are also possible. The device performance can be compared to other works like [6-8] and it can be followed that the sensor is even suitable for applications like in-screen fingerprint applications. In [5] we have shown that the photodiodes exhibit a very fast response time smaller than 10 µs, as would be expected of Schottky-diodes. Using laser illumination at a wavelength of 540 nm the noise equivalent power of the photodiodes could be determined to a value of NEP = 1.96e-10 W/√Hz.

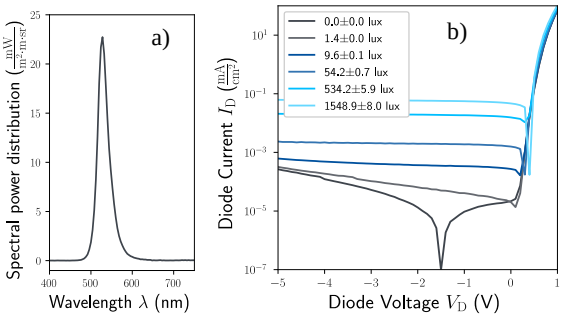

Figure 3. Spectrum of green LED used for illumination for a brightness of 1430 lux (a) and IV-characteristic of photodiode for different illumination levels using the shown LED light at a center wavelength of 520 nm (b).

4. Scalable solutions for array integration

To simplify the driving of the sensor array and demonstrate the scalability of the technology, row drivers were integrated in the presented TFT technology. The chosen architecture is that of the dynamic shift-register with a dedicated output stage shown in [9]. Figure 4 shows the circuit diagram of one driver cell. The Clk1 and Clk2 connections alternate from one cell to the next. The signals required for the driving of this circuit are Clk1 and Clk2, which are the clock and inverted clock signals, as well as an input trigger, a reset signal and a reference potential V_{off}.

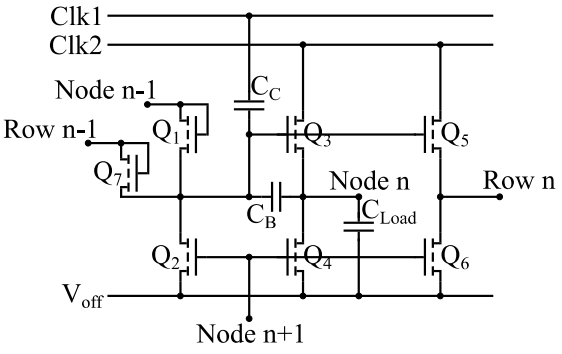

Figure 4. Circuit diagram of one stage of the row driver.

The gate drivers were implemented with a transistor width of w = 100 µm and length l = 10 µm for all transistors. The target line frequency for the driver is 2.5 kHz and the dimensioning and layout take this into account. This relatively low operating frequency is due to the speed limitation set by the current sensing ADC that performs the sensor readout.

5. Sensor array readout platform

A 32 x 32 sensor element active-matrix with integrated row drivers and 4 x-column multiplexing was manufactured using the outlined process. Driving and readout of the active-matrix is done using a microcontroller and a current-input ADC by Texas Instruments (DDC118). Control signals from the microcontroller pass a level shifter to adjust the 0-5V logic levels to 0-20 V. This enables the driving of the integrated driver and multiplexer. The multiplex function is achieved by switching each output line between four columns via dedicated column-selection-TFTs. The matrix thus requires the five signals for the row-drivers, four signals for the multiplex functions and one ADC connection for every four columns of the array. Figure 5 shows an overview of the complete system with all driver and readout components. The reverse bias voltage V_{CC} of the photodiodes is adjustable and was set to a voltage of approximately 3 V for initial operation.

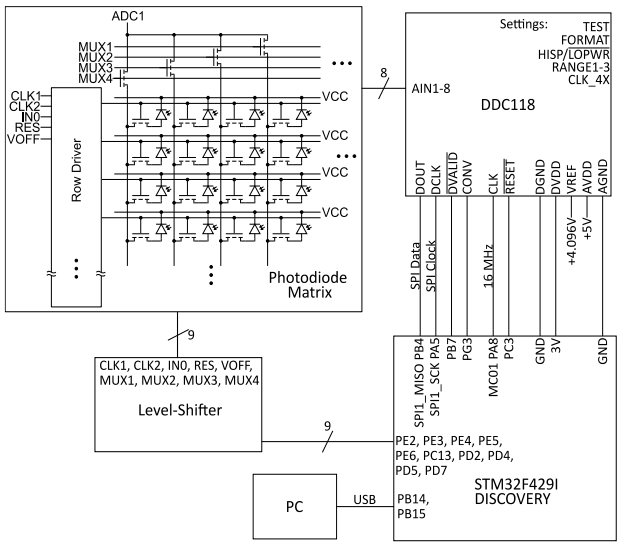

Figure 5. Complete system overview of sensor array, driver circuits as well as control and readout platform.

The layout of the array features a redundant pair of the row drivers to increase yield in our university clean room laboratory. The pixel-TFT has a width and length of 10µm. The pitch of the sensor pixels is 275 µm. The speed of the array readout is limited by the minimal integration time of 400 µs required by the ADCs. Since eight channels can be measured in parallel, this allows for a refresh rate of the sensor image of 19.5 Hz. The integration time also determines the clock frequencies for the row driver. The readout of the ADC is done by a microcontroller via SPI. The controller sorts the data and sends a comprehensive image to a computer via USB, where the data can be further processed. Figure 6 shows screenshots from a live visualization application running on a Windows PC. Obviously, the signal processing could also be performed on typical mobile smart devices instead. In a first setup, an image was printed on foil and placed on top of the sensor array. This setup was illuminated with a broad-spectrum light by a desk lamp from the front side. The resulting array readout can be seen in figure 6b). In a second setup, light entered from the rear of the array and

pictures printed on paper were placed on top of the array. The shown array readout in figure 6c) is the signal resulting from light reflected by the paper back onto the sensor array. Pixel defects from manufacturing usually appeared as shorted photodiodes, resulting in hot pixels that also affect the readout of the next two pixels in the column. Such defects have been removed from the image by setting their value as the average of the neighboring pixels. Figure 6a) shows the comparison between sensor readout with and without the removal of hot pixels.

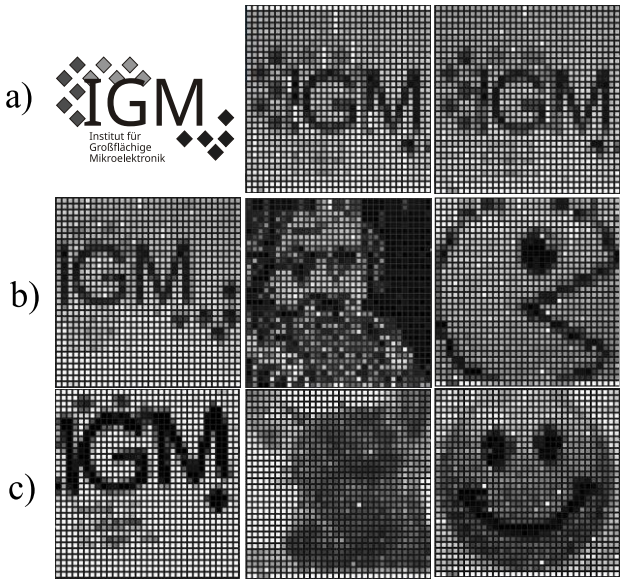

Figure 6. Screenshot of live readout from photosensor array. Row (a) with vectorized logo and a comparison of an uncompensated (middle) and compensated (right) image with regard to hot pixels. For row (b) the image is illuminated from the top side and images, printed on transparent foil are placed on the array. Row (c) shows the setup with the array illuminated from the back side, with images on paper placed on top of the array.

6. Conclusion

We developed a process for the co-fabrication of a-Si:H Schottky photosensors as well as a-Si:H TFTs that requires only one additional functional layer. Device performance shows great promise for use in a wide variety of applications from ambient light sensing for dynamic spatially resolved brightness adjustment of displays to biometric functionality like in-screen fingerprint detection. Using this process, an active-matrix of photosensors was produced, featuring integrated drivers and column multiplexing for reduced external circuitry and demonstration of a scalable design. Live readout of the array is shown using a simple driver platform.

7. Acknowledgements

Parts of this work were funded by Kepler Corp, Tokyo.

8. References

1. Lin CY *et al.*, “Ambipolar Gap-type a-Si-TFT Circuit Applied for a Color Ambient Light Sensor.” Digest of Technical Papers - SID International Symposium. 2023;54(1):676-679. doi: 10.1002/sdtp.16649.
2. S. S. Tan *et al.*, “Spectral response design of hydrogenated amorphous silicon p-i-n diodes for ambient light sensing.” In Applied Physics Letters 94, Apr. 2009, doi: https://doi.org/10.1063/1.3125250.
3. A. Cho *et al.*, “In-Cell Ambient Light Sensors (ALSs) LCD Integration Using a-Si TFT photo-transistor and Four-Mask Process Architecture Technology.” Digest of Technical Papers - SID International Symposium. 2023, 54: 684-687. https://doi.org/10.1002/sdtp.16651.
4. Siewerdsen, J. H., Antonuk, L. E. *et al.* „Empirical and theoretical investigation of the noise performance of indirect detection, active matrix flat-panel imagers (AMFPIs) for diagnostic radiology.” *Medical physics* **24**, 71-89, doi:10.1118/1.597919 (1997).
5. Dettling, M. M. *et al.* “Large-Area Hydrogenated Amorphous Silicon Schottky-Photosensor Arrays for Display Integration.”, In proceedings of Eurodisplay2024
6. Bae, K. S. *et al.*, “Full Screen Fingerprint Display with Embedded Organic Photo-detectors.”, SID Symposium Digest of Technical papers, 2024, 55: 142-145, doi: https://doi.org/10.1002/sdtp.17474
7. Kamada, T., *et al.* , “OLED/Organic Photodetector Dual-Mode Device Integrated into Side-by-Side Patterned OLED Display.”, SID Symposium Digest of Technical Papers, 2024, 55: 146-149., doi: https://doi.org/10.1002/sdtp.17475
8. Zhou, L., *et al.*, “Ultrasensitive Image Sensor Based on Amorphous Silicon Avalanche Photodiodes (a-Si APD) Used for Optical Fingerprint Identification and Flat-panel X-ray Detector.”, SID Symposium Digest of Technical Papers, 2024, 55: 1003-1006., doi: https://doi.org/10.1002/sdtp.17706
9. Schalberger, P., Baur, H., Bürgstein, T., Fruehauf, N.: A Low Mask Count Top Gate Process for AMOLED Displays Based on Amorphous or Polymorphous Silicon. Digest IDW’09, pp. 463-466, Paper OLED3/AMD3-2 (December 2009). (2009).